Applied Physics B (2018) 124:9
https://doi.org/10.1007/s00340-017-6877-6

Applied Physics B
Lasers and Optics

Tunable, high-repetition-rate, dual-signal-wavelength femtosecond optical parametric oscillator based on BiB_3O_6

Xianghao Meng[1,3] · Zhaohua Wang[1] · Wenlong Tian[2] · Shaobo Fang[1] · Zhiyi Wei[1]

Received: 9 November 2017 / Accepted: 5 December 2017 / Published online: 19 December 2017

Abstract
We have demonstrated a high-repetition-rate tunable femtosecond dual-signal-wavelength optical parametric oscillator (OPO) based on BiB_3O_6 (BiBO) crystal, synchronously pumped by a frequency-doubled mode-locked Yb:KGW laser. The cavity is simple since no dispersion compensators are used in the cavity. The wavelength range of dual-signal is widely tunable from 710 to 1000 nm. Tuning is accomplished by rotating phase-matching angle of BiBO, and optimizing cavity length and output coupler. Using a 3.75 W pump laser, the maximum average dual-signal output power is 760 mW at 707 and 750 nm, leading to a conversion efficiency of 20.3% not taking into account the idler power. Our experimental results show a non-critical phase-matching configuration pumped by a high peak power laser source. The operation of the dual-signal benefits from the balance of phase matching and group velocity mismatching between the two signals.

1 Introduction

Simultaneous multi-wavelength laser sources, especially femtosecond dual-wavelength lasers are applied in various fields of pump–probe measurements [1], difference-frequency terahertz-wave generation [2, 3], coherent combination [4] and optical waveform synthesis [5]. Especially in the field of military, multi-wavelength laser are of great interest for a variety of applications including laser range, coherent laser radar and laser communications. For instance, eye-safe optical parametric oscillators (OPOs) with wavelength tunable have been proven to be useful in laser range due to high conversion efficiency and high energy. The dual-wavelength ultrashort pulses are produced generally from mode-locked lasers based on solid-state or fiber gain medium, such as ytterbium-doped yttrium aluminum garnet (Yb:YAG), titanium-doped sapphire (Ti:Sapphire), Yb-doped and Er-doped fiber. In 1993, Evans et al. have introduced dual-wavelength operation based on mode-locked Ti:sapphire lasers [6]. Several years later, Pudo et al. have generated actively mode-locked tunable dual-wavelength Er-doped fiber lasers [7]. In 2010, Yoshioka et al. have reported a dual-wavelength independently mode-locked Yb:YAG ceramic laser in a single cavity [8]. By 2012, Zhang et al. have demonstrated a dual wavelength dissipative solitons in an all-normal-dispersion mode-locked Yb-doped fiber laser [9]. With these methods, however, the output dual-wavelength pulses are limited by the gain medium, lying in the near infrared and visible spectra regions. In addition, the phase of dual-wavelength is not locked although the synchronization precision is high. Over the last decade, many nonlinear optics crystals, such as $KTiOPO_4$ (KTP), $KTiOAsO_4$ (KTA), β-BaB_2O_4 (BBO), LiB_3O_5 (LBO), BiB_3O_6 (BiBO), $MgO:LiNbO_3$ (PPLN) have been employed for the ultrashort pulses generation through synchronously pumped OPOs [10–21]. Own to high power density and good spatial mode matching in the cavity, high power and high conversion efficiency tunable femtosecond dual-wavelength with good beam quality can be generated from the OPOs. In this method, synchronization and phase lock of two independent femtosecond lasers are proved to generate efficient tunable sources for precision frequency measurements based on optical frequency comb. Furthermore, it

✉ Zhaohua Wang
zhwang@iphy.ac.cn

✉ Zhiyi Wei
zywei@iphy.ac.cn

[1] Beijing National Laboratory for Condensed Matter Physics, Institute of Physics, Chinese Academy of Sciences, Beijing 100190, China

[2] School of Physics and Optoelectronic Engineering, Xidian University, Xi'an 710071, China

[3] University of Chinese Academy of Sciences, Beijing 100049, China

can also be used for difference-frequency terahertz-wave generation because the dual-signal-wavelengths are close to each other. In previous reports, the using of coherent pulse synthesis by the electronic feedback is a feasible method to obtain synchronization and phase-locking dual wavelength. In 2008, Reid et al. have reported two coherent pulse by locking the carrier-envelope phase-slip frequencies of pulses from a synchronously pumped femtosecond OPO and its pump laser [22]. Next year, Sun et al. have achieved coherent pulse synthesis between the pump and second harmonic (SH) signal pulses with a phase coherence 1.4 ms, and the mutual timing jitter of 30 as in 20 ms [23]. Similarly, the best choice of immediately generating femtosecond dual-signal-wavelength is to control the pulses operating close to the net-zero group velocity dispersion (GVD). In 1997, Burr et al. have reported high-repetition-rate femtosecond dual-signal based on PPLN by optimizing intracavitary dispersion [24]. Recent years, the Yb-doped solid-state oscillator and Yb-doped fiber amplifier offer new attractive properties for synchronously pumped femtosecond OPOs owing to good beam quality, high power and low cost. Utilizing the typical dual-signal-wavelength phase-matching property of nonlinear optics crystals is a feasible method to achieve femtosecond dual-signal-wavelength operation. In 2014, Gu et al. have demonstrated a femtosecond dual-signal-wavelength OPO based on a temperature turned LBO [11]. Similar theoretical calculated results also obtained on BBO OPO when the pump laser is centered at 520 nm. Compared with LBO and BBO, the BiBO is rapidly emerging as a highly attractive alternative due to its outstanding optical properties for frequency conversion in the visible and near-infrared. The effective nonlinear coefficient of BiBO is nearly twice and four times larger than those of BBO and LBO under the same condition, which is comparable to KTP. At the same time, BiBO also offers large phase-matching bandwidth and broadband angle tuning at room temperature, which can support dual-signal-wavelength operation in femtosecond OPOs.

In this letter, we have reported synchronously pumped high-repetition-rate femtosecond OPO based on BiBO crystal with tunable dual-signal operation. The tunable dual signal within the wavelength range from 710 to 1000 nm has been produced. The total signal power is 760 mW at wavelength 707 and 750 nm, corresponding to the conversion efficiency of 20.3% using a 3.75 W pumping laser, which not including the idler power. The experimental results indicate the conditions of phase-matching are not quite strict under high peak power pump source. Except for controlling the net-zero dispersion, the balance of the group velocity matching (GVM) and phase-matching condition between dual-signal is another important effect to support femtosecond dual signal operation.

2 Experiment setup

The experimental setup of BiBO OPO system for tunable femtosecond dual-signal generation is shown in Fig. 1. A femtosecond mode-locked Yb:KGW oscillator is used as the pump source with a pulse duration of 90 fs at 75.5 MHz repetition rate. The maximum average power is 7 W at the central wavelength of 1030 nm. The LBO crystal is cut at $\theta = 90°$, $\phi = 13.6°$ for type I phase matching in the optical xy-plane ($o + o \rightarrow e$) with a length of 2.4 mm, coated with high transmittance at 1030 nm and 515 nm on the both end faces. The pump beam is focused into the center of LBO crystal by a 100-mm focal lens (L1) and followed by a 150-mm focal length collimating lens (L2). Two dichroic mirrors (DM) spectrally separate the green pulses (reflecting) and the remaining pump pulses (transmitting). A half wavelength plate (HWP2) and a polarizing beam splitter (PBS) are employed as variable attenuator to change the power of the green pulses. The HWP3 is used to adjust the polarization direction for the optimum phase-matching directions in the BiBO crystal. The green pump pulses are focused into the BiBO crystal through a lens (L3) with 150 mm focal length. The BiBO OPO system is based on a linear cavity and consists of two concave spherical mirrors, C1 (150 mm ROC) and C2 (100 mm ROC), two high reflection mirrors (HR1, HR2) and an 11% plane output coupler (OC). All the mirrors have a high reflection coating ($R > 99.9\%$) over 620–1120 nm range. In addition, the transmission coating of C1 and C2 are higher than 95% between 488 and 532 nm. The total length is set to about 993 mm corresponding to the repetition rate of 151 MHz which is equal to double of that of the Yb:KGW oscillator. A 174°-cut, 2.4-mm-long BiBO crystal is used as the nonlinear gain medium for type I phase matching in the optical yz-plane ($o \rightarrow e + e$), which is coated by an antireflection

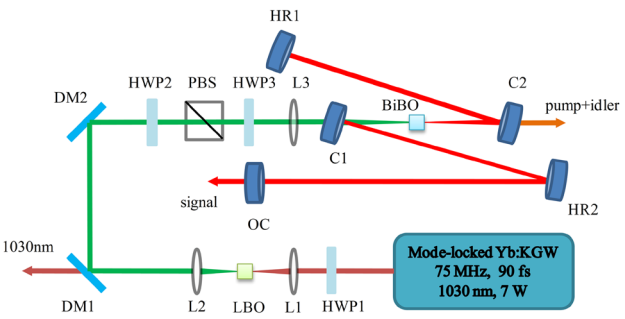

Fig. 1 The schematic diagram of femtosecond dual-signal in BiBO OPO. *L1, L2* and *L3* focal lens, *HWP1, HWP2* half wavelength plate, *PBS* polarizing beam splitter, *C1, C2* concave spherical mirrors, *DM1, DM2* dichroic mirrors, *HR1, HR2* plane mirrors, *OC* 11% output coupler

(AR) coating on both surface over 700–1400 nm and high transmission coating at the 510–530 nm.

3 Experimental results and discussions

Among the nonlinear crystals, LBO is employed for the generation of second harmonic (SH) pulse owing to high nonlinear coefficient, high optical damage and small walk-off. Under a 7 W infrared pump power, the maximum power of SH pulses as high as 3.75 W is obtained at the central wavelength of 515 nm, corresponding to the conversion efficiency up to 53.6%. By focusing the 515 nm pump beam into the BiBO crystal, the stable dual-signal pulses are achieved when the cavity length of BiBO-OPO system is matched to the half of that of Yb:KGW laser. In our experiment, the total maximum output power is 760 mW at 707 and 750 nm corresponding to the pump-to-signal conversion efficiency of 20.3%. Figure 2 shows the long-term power stability of the dual-signal-wavelength output from the OPO. The dual signal is recorded to exhibit natural stable with a fluctuation of 1.9% rms in 1 h, while operating a maximum output power of 760 mW. For comparison, the simultaneously measured SH power exhibits a stability better than 0.2% over the 3 h, as inserted in Fig. 2. The fluctuation of power stability is due to the perturbation of the environment around, such as air turbulence and lab vibration, which can be effectively resolved using active feedback control and isolation. As shown in Fig. 3, by turning the cavity length, we could change the signal spectra during the dual-signal operation. From (a) to (e), first the dual-signal is operation at 695 and 764 nm. Then, the two distinct signal approach gradually by the edge to the center when the cavity length is continuously

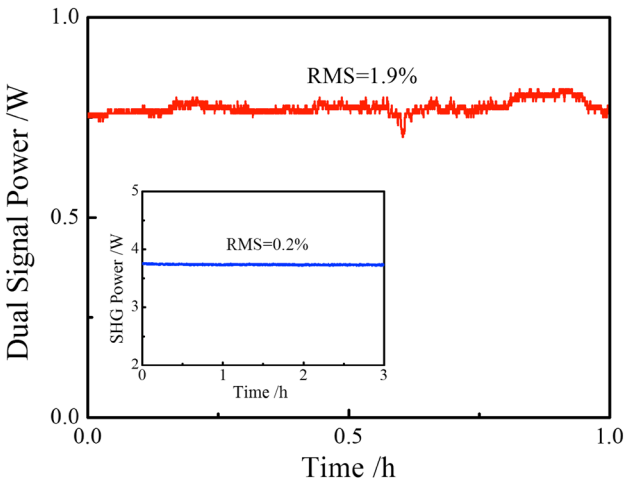

Fig. 2 Long-term power stability of the maximum output power for 1 h at the wavelength of 707 and 750 nm. Inset: power stability of the SHG power in 3 h

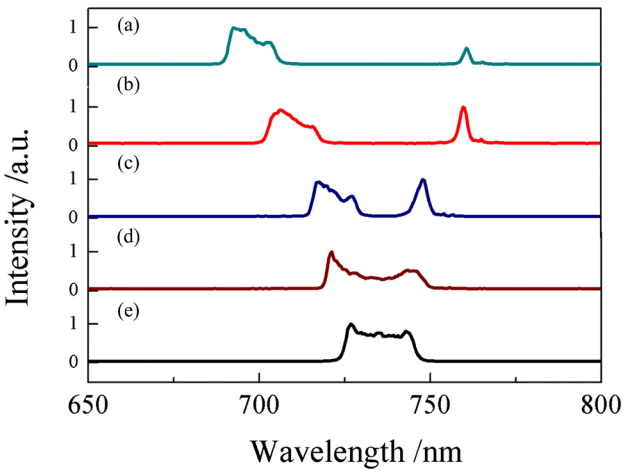

Fig. 3 Dual-wavelength spectra of the signal pulse. **a**–**e** Shows the changing process of signal when the cavity length is continuously shorted

shorted. Finally, they are integrated as a single wavelength at 733 nm. The similar results have been reported in the femtosecond PPLN OPO systems. The generation of dual-wavelength is possible by controlling the net GVD for two different signal in the cavity [24]. However, in our experiment, the 2.4-mm-long BiBO is the primary dispersive medium and other mirrors provide no dispersion compensation. The operation of dual-signal cannot be achieved around 0 GVD region. The phase-matching condition is not quite rigor using high peak power pump laser pulses. The balance of phase-matching condition and GVM between dual signals is more significant for generation of dual-signal. The dual signal lag behind the pump pulse due to the GVM between the interacting waves, and they are broadened to longer pulse durations than the pump laser pulses. A 2.4-mm-long BiBO introduces a large GVM between pump and signal pulses. When the dual-signal operate at wavelength of 723 and 748 nm, the GVM are 248 and 264 fs between signal and pump pulses, respectively. It means the time delay is 16 fs between dual signals, which indicate they can overlap partly with pump pulses. It is confirmed by the fact that the dual-signal output power is almost equally shared and the difference is below 10%. As the cavity length is lengthened gradually, the spectral intervals increase and the delay time become longer between dual signals. As shown in Fig. 3a, the spectral intervals of dual-signal is about 60 nm and the GVM is 208 and 288 fs at the wavelength of 695 and 764 nm, respectively. The delay time between dual signals is 80 fs which is almost equal to the pulse duration of the pump. In this model operation, one of signals meets good phase matching condition but suffers from large GVM. At the same time, another signal is overlapped well with pump pulse but meets weak phase-matching condition [25].

Utilizing the balance between the phase-matching condition and GVM, the net gain experienced of dual signal proved to be comparable so that they can oscillate simultaneously. When the balance is broken, the operation of dual-signal disappear and the single wavelength occurs.

The pulse durations of dual-signal are measured by an intensity autocorrelation. The corresponding intensity autocorrelation trace is shown in Fig. 4, which proves clearly the synchronization and the coherence between dual signals. It is obvious that the trace has two large side peaks which exist all the time in the case including a large GVD. The two side peaks are generated through sum-frequency mixing for 723 and 748 nm, which indicates the dual signals are temporary separated. Accordingly, the central peak is the overlap of the SH for the 723 and 748 nm. The pulse durations of side peak and central peak are 83 and 71 fs, respectively. The corresponding dual-signal spectrum centered at 723 and 748 nm is shown in the inset of the Fig. 4. However, the wavelength of dual signal are quite close to each other so that the difference in phase matching angles for SH generation of individual signal is just 1.2° in BBO crystal. In this reason, the measurement of pulse duration for each signal is not possible by this traditional intensity autocorrelation. As further shortness of the OPO cavity length, the operation of dual-signal disappears because the balance of phase matching condition and GVM is broken. Then stable single-wavelength is achieved. The output power of single wavelength as high as 1.2 W is obtained at 728 nm and the conversion efficiency is 32% not taking into account the idler power. Figure 5 depicts the intensity autocorrelation trace and the corresponding spectra of single-wavelength at the central wavelength of 728 nm. Assuming a $sech^2$ pulse

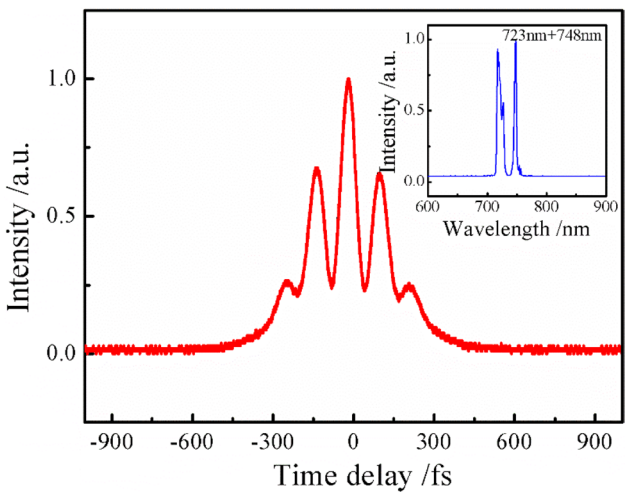

Fig. 4 Intensity autocorrelation trace of the dual-signal when the wavelength is operation at 723 and 748 nm. Inset: corresponding to spectra of dual signal

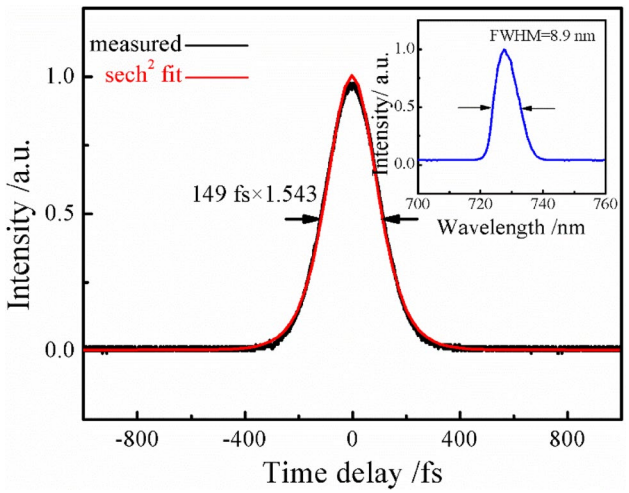

Fig. 5 Intensity autocorrelation trace of single-wavelength at 728 nm and inset: corresponding to signal spectra

shape, the pulse duration is 149 fs. The corresponding full width at half maximum (FWHM) is about 8.9 nm. These result in the time-bandwidth product of 0.75 increased by 1.38 times from the Fourier limit for a $sech^2$ pulse (0.315), which indicates a big residual chirp exists without any dispersion compensation elements in the OPO cavity.

As shown in Fig. 6, the tunable dual-signal in the range of 710–1000 nm can be obtained through OPO system by appropriately rotating the phase matching angle of BiBO crystal, adjustment of the cavity length and OC mirror. The maximum and minimum wavelength spacing of dual-signal is 695 to 764 nm and 906 to 930 nm, respectively. The maximum wavelength spacing is close to 50 nm and the minimum wavelength is just two dozen nanometers within the entire wavelength turning range. The output power of dual-signal is greater than 500 mW of the tuning range (710–930 nm) and the pump-to-signal power extraction efficiency is more than 13%. However, in the wavelength range of 930–1000 nm, the power is just about 250 mW. This results can be explained that the operation of dual-signal is close to point of degeneracy, and the mode competition between the signal and idler is intense due to the associated doubly resonant oscillation. In addition, other second-order nonlinear optical phenomenon such as SH generation also be present along with OPO. The blue light at the SH of the infrared signal has been observed and measured at the non-phase matching angle. When the signals operate at wavelength between 790 and 840 nm, the output power decreases as the intracavity power is converted into generating blue light which is tunable from 395 to 420 nm. An obvious blue light is observed on the HR1 and a similar facular has been produced in the opposite direction on the OC mirror. Unfortunately, the output power is not able to measure without high transmission coating nearby 400 nm on the each mirror.

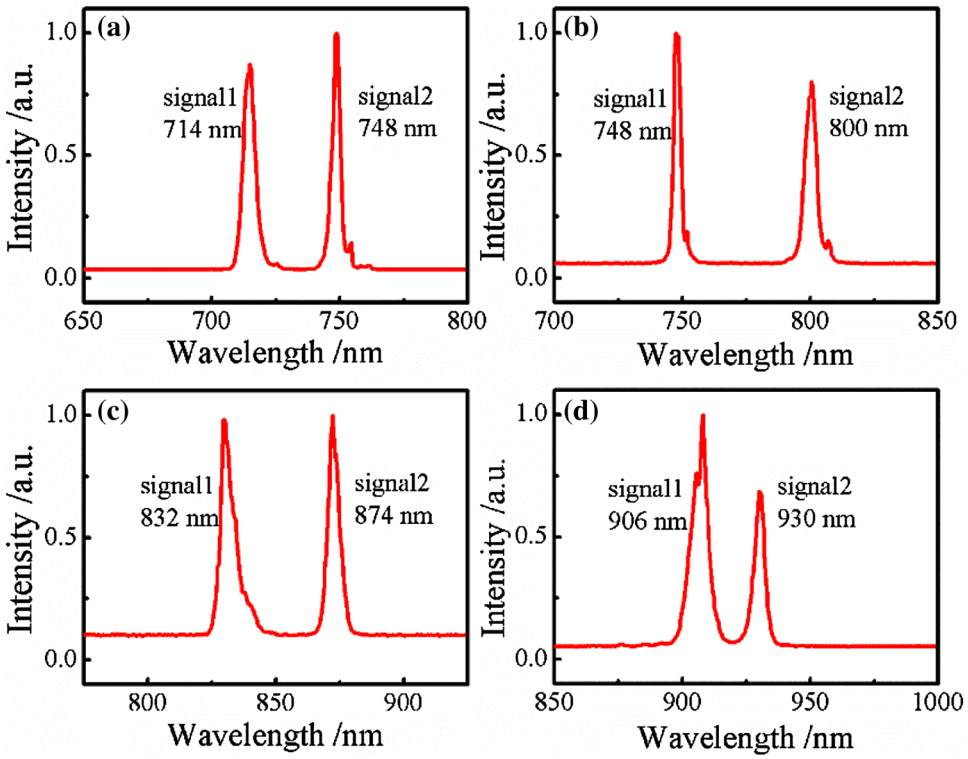

Fig. 6 The typical dual signal spectra of BiBO OPO

4 Conclusion

In conclusion, we have demonstrated high-repetition-rate dual-signal operation based on BiBO crystal synchronously pumped by a frequency-doubled mode-locked Yb:KGW laser, without any dispersion compensation elements in the OPO cavity. With a 3.75 W of pump power at 515 nm, the maximum output power is 760 mW at the wavelength 707 and 750 nm, corresponding to the pump-to-signal conversion efficiency of 20.3%. The OPO dual-signal is tunable from 710 to 1000 nm by rotating the phase matching angle of BiBO crystal, adjustment of the cavity length and OC mirror. The operation of dual-signal benefits from the high peak power of pump laser. It is worth noting that the balance of the phase matching condition and GVM is important between the dual signals. Owing to the better synchronization and the coherence, the dual-signal OPO may be well suit for many potential applications in the ultrafast optics, such as difference frequency generation of terahertz, double-pulse pump–probe measurements and coherent control.

Acknowledgements We thank the funding supported by the National Key Scientific Instruments Development Program of China (2012YQ120047), the National Natural Science Foundation of China (61575217, 61575219 and 11774410), the Strategic Priority Research Program of Chinese Academy of Sciences (XDB16030200), the National Key R&D Program of China (2017YFC0110301) and the Key Research Program of Frontier Sciences of Chinese Academy of Sciences (KJZD-EW-L11-03).

References

1. G.M. Gale, G. Gallot, F. Hache, N. Lascoux, S. Bratos, J.-C.L. Leicknam, Phys. Rev. Lett. **82**, 5 (1999)
2. K. Kurokawa, M. Nakazawa, Appl. Phys. Lett. **55**, 7 (1989)
3. C. Phillips, J. Jiang, C. Mohr, A. Lin, C. Langrock, M. Snure, D. Bliss, M. Zhu, I. Hartl, J. Harris, M. Fermann, M. Fejer Opt. Lett. **37**, 2928–2930 (2012)
4. S.W. Huang, G. Cirmi, J. Moses, K.H. Hong, S. Bhardwaj, J.R. Birge, L.J. Chen, E. Li, B.J. Eggleton, G. Cerullo, F.X. Kärtner, Nat. Photonics **5**, 8 (2011)
5. Y. Kobayashi, H. Takada, M. Kakehata, K. Torizuka Opt. Lett. **28**, 1377–1379 (2003)
6. J.M. Evans, D.E. Spence, D. Burns, W. Sibbett, Opt. Lett. **8**, 13 (1993)
7. D. Pudo, L.R. Chen, D. Giannone, L. Zhang, I. Bennion, IEEE Photon. Technol. Lett. **14**, 2 (2002)
8. H. Yoshioka, S. Nakamura, T. Ogawa, S. Wada, Opt. Express **18**, 2 (2010)
9. Z.X. Zhang, Z.W. Xu, L. Zhang, Opt. Express **20**, 24 (2012)
10. F. Ganikhanov, S. Carrasco, X.S. Xie, M. Katz, W. Seitz, D. Kopf, Opt. Lett. **31**, 9 (2006)
11. C. Gu, M. Hu, J. Fan, Y. Song, B. Liu, C. Wang, Opt. Lett. **39**, 13 (2014)
12. F. Kienle, P.S. Teh, D. Lin, S. Alam, J.H.V. Price, D.C. Hanna, D.J. Richardson, D.P. Shepherd, Opt. Express **20**, 7 (2012)
13. T. Lang, T. Binhammer, S. Rausch, G. Palmer, M. Emons, M. Schultze, A. Harth, U. Morgner, Opt. Express **20**, 2 (2012)
14. M. Ghotbi, A.E. Martin, M.E. Zadeh, Opt. Lett. **33**, 4 (2008)
15. M. Wang, L. Zhu, W. Chen, D. Fan, Opt. Lett **37**, 13 (2012)
16. A. Zavadilová, V. Kubeček, J. Diels, Laser Phys. Lett. **4**, 103–108 (2006)
17. Y. Jin, S.M. Cristescu, F.J.M. Harren, J. Mandon, Opt. Express **23**, 16 (2015)

18. V.R. Badarla, A.E. Martin, M.E. Zadeh, Opt. Lett. **40**, 3 (2015)
19. W. Tian, Z. Wang, X. Meng, N. Zhang, J. Zhu, Z. Wei, Opt. Lett. **41**, 4851 (2016)
20. A. Zavadilová, V. Kubeček, J. Diels, J. Šulc Laser Phys. Lett. **8**, 839–844 (2011)
21. T. Ferreiro, J. Sun, D.T. Reid, Opt. Lett. **35**, 10 (2010)
22. B.J.S. Gale, J.H. Sun, D.T. Reid, Opt. Express **16**, 3 (2008)
23. J.H. Sun, D.T. Reid, Opt. Lett **34**, 6 (2009)
24. K.C. Burr, C.L. Tang, M.A. Arbore, M.M. Fejer, Appl. Phys. Lett. **70**, 3341 (1997)
25. L. Xu, X. Zhong, J. Zhu, H. Han, Z. Wei, Opt. Lett. **37**, 9 (2012)